Design of a High Performance Patch Antenna for GPS Communication Systems

Sotoudeh Hamedi-Hagh*, Joseph Chung*, Sooseok Oh*, Ju-Ung Jo, Noh-Joon Park and Dae-Hee Park†

Abstract – This paper presents the design of a patch antenna for GPS portable devices. The antenna is designed to operate at L1 band on an FR4 PCB with a thickness of 1.6mm, a dielectric constant of 3.8 and two metallization layers. The antenna has a dimension of 49mmX36mm and operates at 1.5754GHz with a return loss of |-36|dB and a measured bandwidth of 250MHz.

Keywords: Patch Antenna, GPS, L-ground, h-type

1. Introduction

Advances in portable handheld wireless devices create a demand for combining many features onto a single PCB. Global positioning systems (GPS) are one of the most useful capabilities that are being integrated with many other wireless devices. GPS satellites are located at far distances and design of a high performance antenna is crucial in detecting weak signal levels and improving the performance of a receiver.

The theory and design of the GPS antenna through characterizations of the FR4 PCB are discussed in section II. This section will mainly focus on design of the "L-ground h-type configuration with cornered patch structure. Section III represents the simulation and measurement results and finally, section IV concludes the paper.

2. GPS Antenna

Technically, the GPS has two services, the Precise Positioning Service, PPS, for the military and the Standard Positioning Service, SPS, which is less accurate, but still very effective for civilians [1]. SPS transmits messages on to the L1 signal at the carrier frequency of 1575.42MHz with a bandwidth of 2.046MHz and with right hand circular polarization [1]. This paper will focus on the L1 civilian frequency.

After showing the preference of using PCB over silicon for antennas, the analysis and design will be discussed, followed by simulation and measurement results of the "L-ground h-type configuration with cornered patch" GPS antenna.

2.1 PCB over Silicon Antenna

PCB FR4 antenna offer low cost and high efficiency as listed in Table 1. Also, high performance silicon antennas are much more complex to fabricate compared to PCB. The typical range of the dielectric of PCB is much less than the counterpart of silicon substrates, which allows for greater radiation.

Table 1. PCB Antenna vs. Silicon Antenna

	Silicon Antenna	FR4 PCB Antenna
Area/Cost	High	Low
Fabrication Complexity	High	Low
Radiation Efficiency	Low	High
Dielectric Constant	High	Low

The antenna design and analysis on FR4 PCB are presented in the next section.

2.2 Analysis and Design

A starting point to design a reasonable small antenna is the classic inverted-F [2-3] due to its compactness. After analyzing the parameters such as polarization and radiation patterns, a modified antenna design is proposed. The proposed antenna is a unique "L-ground h-type configuration with cornered patch" shown in Fig. 1.

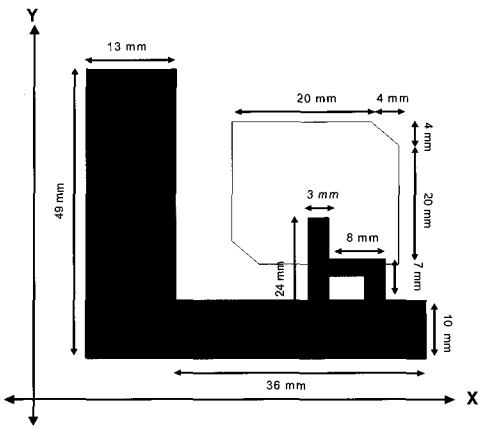

Fig. 1. Proposed Geometry of Antenna

† Corresponding Author: Department of Electrical, Electronic & Information Eng., Wonkwang University, 344-2 Shinyoung-dong, Iksan, 570-749, Korea. (parkdh@wonkwang.ac.kr)
* Sotoudeh Hamedi-Hagh, Soo-Seok Oh, and Ahmet Bindal are form RFIC Research Lab, San Jose State University, San Jose, CA 95192-0084, USA
Received 14 July 2008; Accepted 14 April 2009

The influences due to the radiation pattern, the directivity, the gain, the polarization, and finally the impedance bandwidth with the Q-factor will be explained for the proposed geometry in Fig. 1.

Although radiation patterns define an antenna's electric field characteristics, the explanations can be based on various models. One particular method to determine the radiation pattern is based on the electric surface current model, which for rectangular patches would be [4]

$$E\varphi(\theta,\varphi) = \sin\varphi\left(\frac{j\omega\mu_0}{4\pi r}\right)e^{-jk_0 r}(CurrentCha\ r)(GndEff) \quad (1)$$

and

$$E\theta(\theta,\varphi) = -\cos\varphi\left(\frac{j\omega\mu_0}{4\pi r}\right)e^{-jk_0 r}(CurrentChar)(GndEff) \quad (2)$$

The radiation pattern can be observed to be highly dependent on r, the distance, μ_0, the permeability free space, and k, the wave number. The term "*CurrentChar*" is the current characteristic and "*GndEff*" is the ground effects and substrate contribution term. Both mentioned terms are related to the polar coordinates and are highly dependent on the antenna's geometry. The left vertical side of the "L" shaped ground plane along the Y axis in Fig. 1 acts as a unique reflector to create a strong front beam in the +X direction.

The far-field radiation patterns can be found by finding the limit of the electric or magnetic field to infinity, such as through [5]

$$\vec{E}(r\to\infty,\theta,\varphi) = \vec{E}_{farfield}(\theta,\varphi)\frac{e^{-jkr}}{r} \quad (3)$$

and

$$\vec{H}(r\to\infty,\theta,\varphi) = \vec{H}_{farfield}(\theta,\varphi)\frac{e^{-jkr}}{r}, \quad (4)$$

where r, the distance, is shown to have a large influence with the electric and magnetic fields.

Directivity and gain are related from the fact that both depend on the direction of the maximum radiation intensity. Specifically, the directivity can be represented as [19]

$$D(\theta,\varphi) = \frac{4\pi\left(\max\left(\frac{1}{2}\left(E_{farfield}(\theta,\varphi)\times H_{farfield}^{*}(\theta,\varphi)\right)\right)\right)}{\frac{1}{2}\int_{\Omega}E_{farfield}\times H_{farfield}^{*}\cdot d\Omega} \quad (5)$$

Essentially, the direction of the maximum radiation is divided by the average radiated power through the Poynting vector [6], in Watts, to determine the directivity, which is similar to determining the gain [5] in

$$G(\theta,\varphi) = \frac{4\pi\left(\max\left(\frac{1}{2}\left(E_{farfield}(\theta,\varphi)\times H_{farfield}^{*}(\theta,\varphi)\right)\right)\right)}{P_{input}} \quad (6)$$

The difference between the two equations (5) and (6) is in the denominator, where the maximum radiation is relative to either the radiated power or the input power, respectively.

The proposed reflector influenced directivity since the desired goal is to have the main beam at φ = 0° and was achieved by it reflecting the fields opposite of the 180° direction, creating the intense forward power and focused gain.

Another antenna parameter that may be characterized is the polarization behavior for the varying EM vector waves. The initial versions of the proposed antenna exhibited various linear properties, which is modified to create the version with right hand circular polarization.

The innate characteristic of the "h-shape" portion of the antenna without the cornered square patch in Fig. 1 had exhibited linear polarization where the electrical field vector moved along the y-axis while propagating in the z-axis with respect to time as [6]

$$\vec{E} = \vec{a}_y E_o^{+} e^{-jkz} \quad (7)$$

Due to the modification of the antenna, the straight portion of the "h" became the λ/8 wavelength coupled feed into the circular polarization patch.

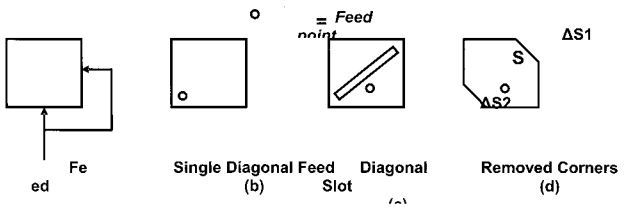

Fig. 2. Various Circular Polarization Patch Methods

Inferring from in Fig. 1, the last mentioned method in Fig. 2(d) is used. The amount of conductor removed, $\Delta S=\Delta S1+\Delta S2$, from the total patch area, S, depends on the circular polarization due to the desired unloaded Q-factor in [4]

$$\frac{\Delta S}{S} = \frac{1}{2Q_o} \quad (8)$$

The phenomenon of the circular polarization of the chosen patch may be explained physically. Removing the two diagonal opposing corners of the square patch creates a 90° phase shift in the exited wave mode creating less capacitance compared to the standard square edges [8]. The patch creates right-hand circular polarization as

$$\vec{E} = E_0(\vec{a}_z - j\vec{a}_y)e^{-jkx} \quad (9)$$

which shows the signal alignment with the Z-Y axes with propagation in the +X direction.

The circular polarization is dependent on the Q-factor as shown in (9) and a correlation to impedance bandwidth will be described. Although the impedance bandwidth can be described as the frequencies in which the antenna transfers power optimally with impedance being well matched, a bandwidth greater than the GPS specification of 2.046MHz ensures full functionality. The design with a greater bandwidth provides a margin of error to safeguard any drifting of the center frequency. The impedance matching at the center frequency in the Fig. 1 antenna is adjusted from the sensitive shorting trace dimensions of h-shape as is similarly for the inverted-F [7-8]. Due to the nature of PCB process variations, to ensure a wide range of matching frequencies, a safe impedance bandwidth of 300MHz is designed with an ideal center at 1.5754GHz for the first iteration.

In terms of the relationship of the bandwidth to the frequency and geometry, the altered square patch portion of

the antenna may be determined through [7]

$$BW \cong 50hf^2 \quad (10)$$

where h is the height of the patch in centimeters, f is the frequency in gigahertz, and BW is the bandwidth in megahertz. After a re-iteration of calculating the bandwidth from grid adjustments, the calculated height was h=2.4cm and the final calculated bandwidth was BW=297MHz using 1.5754GHz as the center frequency.

The calculated bandwidth corresponds to having an impedance matching due to the VWSR equal to 2, which essentially refers to a return loss, RL, of -9.5dB [7]. With the known VSWR, the calculated impedance bandwidth is shown to be correlated to the Q-factor through [4]

$$Q = \frac{\omega W}{P} \quad (11)$$

where W is the energy stored during resonance and P is the power loss. The relation between the BW and Q can be seen through [7]

$$BW = \frac{VSWR - 1}{Q\sqrt{VSWR}} \quad (12)$$

where the BW is inversely proportional to the Q-factor.

3. Simulation and Measurement results

The radiation patterns were only simulated due to the availability of resources; however, the impedance matching and bandwidth were both simulated and compared to the measured results. The fabricated "L-ground h-type configuration with cornered patch antenna" is shown in Fig. 3.

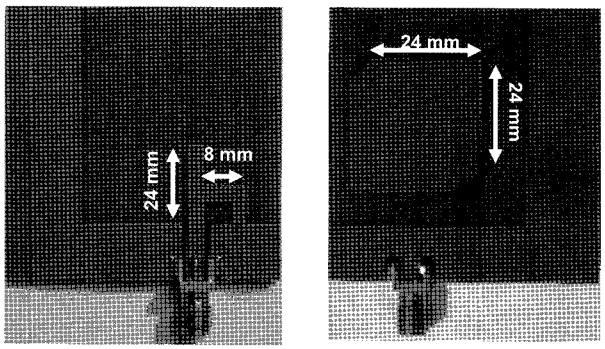

Fig. 3. Front and back pictures L-ground plane with lower-case-h configuration and cornered patch

Fig. 3 shows the front and back of the fabricated antenna. The radiation pattern of the E-field in the φ plane is shown in Fig. 4. The main beam exist at the expected φ = 0° with high intensity between 30° and 330° created by the reflectors.

The corresponding maximum intensity in θ is shown in the ADS antenna dialog in Table 2. The θ angle of directivity for the maximum radiation intensity is 72° as shown in Table 2 with the magnitude shown as 5.00dBi. The direction of radiation is the same for the gain, related through (6), which the ADS simulation shows as 5.01dBi.

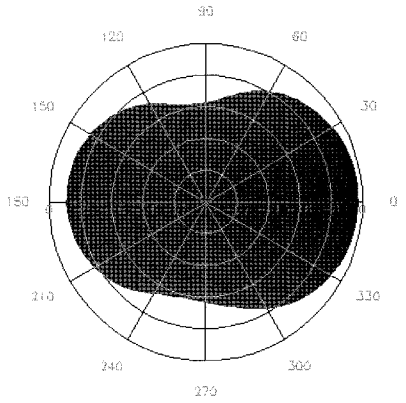

Fig. 4. E-field Radiation Pattern

Table 2. GPS Antenna Characteristics

ADS Antenna Dialog	
Directivity (dBi)	5.01
Gain (dBi)	5.00
Angle of Max radiation intensity (theta, phi)	72, 0

The θ angle vs. the gain displayed in the Sonnet simulation in Fig. 5 shows reasonably similar results regarding the gain at 72°.

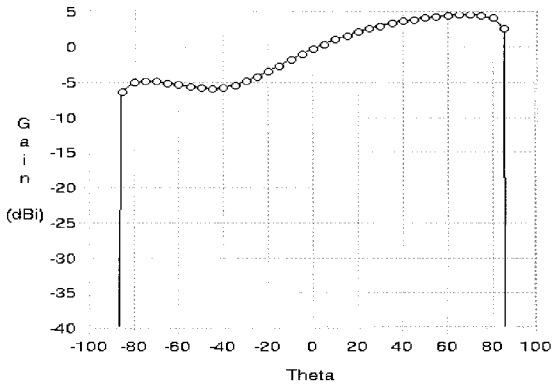

Fig. 5. Sonnet θ vs. Gain

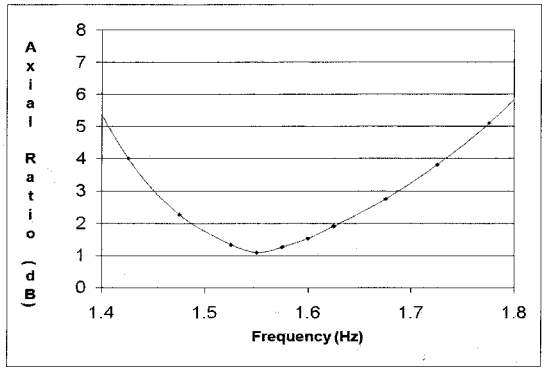

Fig. 6. Right Hand Circular Polarization Pattern

The applications of the radiation oriented antenna in Fig. 5 are versatile, especially useful for portable handheld devices angled with an incline towards the sky. Another antenna parameter is the axial ratio as shown in Fig. 6.

The maximum power is transferred to the antenna when the impedance is matched. The simulated and measured S_{11} results are shown in Fig. 7 and listed in Table 3.

Table 3. GPS Antenna Frequency and Bandwidth

	Goal	ADS	Sonnet	Measured
Δ from center	0	4MHz	25MHz	6MHz
BW	297MHz	75MHz	210MHz	250MHz

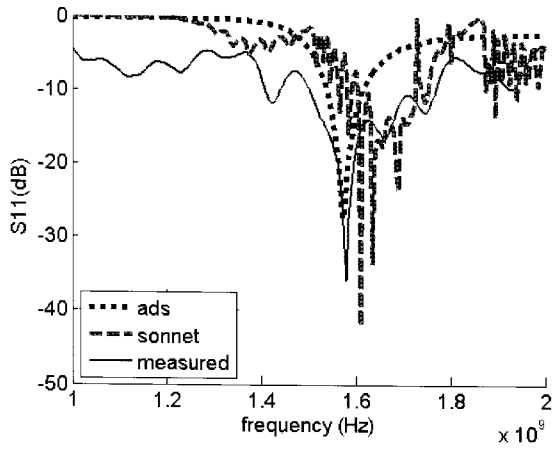

Fig. 7. S11 Parameters with the Simulated and Measured Values

The measured result in Fig. 7 shows that the antenna S_{11} at 1.5754GHz is -36dB, which is sufficient for GPS applications. Compared to the measurement, the ADS simulator presents accurate results in terms of center frequency and the Sonnet simulator presents accurate results in terms of bandwidth profile.

4. Conclusion

The design and measurements of a GPS patch antenna were presented in this paper. The antenna has a dimension of 49mmX36mm and was designed to operate at 1.5754GHz L1 band. It yielded a return loss of -36dB and a measured bandwidth of 250MHz.

Acknowledgment

This work was measured at RFIC research laboratory at San Jose State University. The authors would also like to thank Sonnet Software Inc. and Agilent ADS for providing the use of their tools. And this work was supported by the second phase of the Brain Korea 21 Program in 2009.

References

[1] Global Positioning System Standard Positioning Service Standard, Oct. 2001. Available: http://pnt.gov/public/docs/SPS-2001-final.pdf

[2] Z. Qi, K. Fu, and T.-Z. Liang, "Analysis of planar inverted-F antenna using equivalent models," 2005 IEEE Antennas and Propagation Society International Symposium, Vol. 3A, pp. 142-145, Jul. 2005.

[3] G. Qasim, S. I. A. Shah, and Z. Khan, "Inverted F-Antenna for Mobile Communication," AMPC 2005 Microwave Conference Proceedings, Vol. 5, pp. 4, Dec. 2005.

[4] R. Garg, P. Bhartia, I. Bahl, and A. Ittipiboon, Microstrip Antenna Design Handbook, Norwood: Artech House, Inc., 2001.

[5] Advanced Design System Documentation, Agilent Technologies, Santa Clara, CA, 2004A, ch. 9 pp. 1-12.

[6] D. K. Cheng, "Plane Electromagnetic Waves," Fundamentals of Engineering Electromagnetics, New Jersey: Prentice-Hall, Inc., 1993, ch. 7, sec. 2, pp.272-287.

[6] G. Kumar and K.P. Ray, "An Introduction to Microstrip Antennas" Broadband Microstrip Antennas, Norwood: Artech House, Inc., 2003, ch. 1, sec.5, pp.11-18.

[7] R. Bancroft, "Rectangular Microstrip Antennas," Microstrip and Printed Antenna Design, Atlanta: Noble Publishing Corporation, 2004, ch. 2, sec. 5, pp. 37-48.

Sotoudeh Hamedi-Hagh received his B.A.Sc degree in Electrical Engineering from the Iran University of Science and Technology, Tehran, in 1993 and his M.A.Sc and Ph.D. degrees in Electrical and Computer Engineering from the University of Toronto, Toronto, ON, Canada, in 2000 and 2004, respectively. He joined the faculty at San Jose State University in 2005. His research interests are high frequency modeling of planar and 3-D device structures and design of RF and mixed-signal integrated circuits for wireless communication systems using CMOS and SiGe technologies. Dr. Hamedi-Hagh was the recipient of the best student paper awards at the 2000 Canadian Micronet and the 2004 IEEE Personal, Indoor and Mobile Radio Communication conferences. He holds one U.S. patent in wireless phase shifted transmitter architecture.

Joseph C. Chung (SM'07) was born in San Francisco, California in 1982. He received the B.S.E.E. and M.S.E.E. degrees in electrical engineering from San Jose State University, San Jose, California, in 2005 and 2008, respectively.

Upon completion of his undergraduate

degree, he worked for Compliance Certification Services as an Electromagnetic Compliance Engineer focusing on the regulations of consumer product's wireless bands. He is currently working as a circuit design engineer at Philips/NXP Semiconductors in San Jose, California.

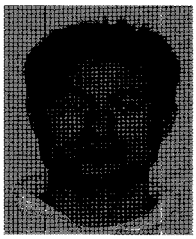

Sooseok Oh

Sooseok Oh received his M.S degree in Electrical Engineering from Mississippi State University, MS, USA in 2000. From 2000 to 2006, he was a Circuit Design Engineer in the Microprocessor Development Group, Intel Corporation, Santa Clara, California. Since then, he has been with Silego Technology, Santa Clara, CA working on analog/mixed-signal design for CMOS PLL clock products. He is currently working toward his Ph.D. through the Gateway Ph.D. program at San Jose State University and Mississippi State University. His main research activities are focused on analog and radio-frequency integrated circuits.

Noh-Joon Park

He received B.S., M.S. and Ph.D. degrees in Electronics Engineering from Wonkwang University in 1993, 1995 and 2004, respectively.

Since 2006, he has been a research professor with Center for Advanced Electric Applications at Wonkwang University working on design and analysis of EM sensors for partial discharge diagnosis in high voltage engineering, electronic circuit design with impedance matching technique for light sources. His research interests include analog integrated circuit design with antenna system, channel measurements and modeling in wireless communication system.

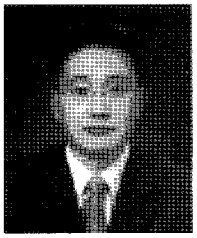

Ju-Ung Jo

He was born on May 27, 1975, in Seoul, Republic of Korea. He got his bachelor's degree from Wonkwang University in Physics & Semiconductor field in March, 2003. He received a B.S. degree in the Department of Electrical Materials, Wonkwang University, Iksan, Korea, in 2005. After graduation, in March, 2005, he joined SE Plasma Inc., which is a atmospheric plasma equipment development in anyang, korea. He is currently taking a doctorial course in the Dept. of Electrical, Electronic & Information Eng., Wonkwang University. His current research focuses on atmospheric pressure plasma source and diagnostic method for blood related diseases using optical imaging and lighting source technical for medicine application. His other research interests include high power LED lighting system and computational modeling of plasma (CFD-ACE) & optic(lightTools).

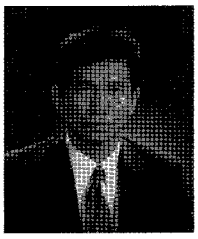

Dae-Hee Park

He was born in 1954 in Korea. He received his B.S. and M.S. degrees in Electrical Engineering from Hanyang University, Seoul, Korea in 1979 and 1983, respectively, and his Ph.D. degree from Osaka University, Osaka, Japan in 1989. He worked at the LG Cable Research Institute as a Senior Researcher from 1979 to 1991. After that, he joined the School of Electrical, Electronics and Information Engineering at Wonkwang University where he is currently employed as a Professor. He has also worked as Director of the "Center for Advanced Electric Application" from 2004 at Wonkwang University. He was at MSU in the USA as a Visiting Professor from 1999 to 2000. His main research interests are in the areas of insulting and dielectric materials, new lighting sources, and discharge. He is a member of the Korean IEE, Korean IEEME, and IEE Japan.